# CHARACTERISATION OF RGS (RIBBON GROWTH ON SUBSTRATE) SILICON MATERIAL AND SOLAR CELLS

G. Hahn, M. Spiegel, S. Keller, A. Boueke, P. Fath, G. Willeke, E. Bucher,
C. Häßler*, H.-U. Höfs*, S. Thurm*
*Universität Konstanz, Fakultät für Physik, P.O.Box X916, D-78457 Konstanz, Germany*
*Tel.: +49-7531-88-3644, Fax: +49-7531-88-3895*
**Bayer AG, Rheinuferstraße 7-9, D-47829 Krefeld-Uerdingen, Germany*
*Tel.: +49-2151-88-5358, Fax: +49-2151-88-7959*
*E-mail: giso.hahn@uni-konstanz.de*

ABSTRACT: The aim of this work was to study the material properties of Bayer RGS Si [1] in order to develop a suitable solar cell process for this low-cost material. The crystal defects present in RGS, which have been investigated in the present work by TEM studies, are in combination with metal impurities and a high oxygen content responsible for the lower solar cell parameters observed so far when compared to standard cast multicrystalline Si. The influence of crystal defects and impurities is also responsible for anomalies in the temperature dependence of the majority charge carrier Hall mobility.
Solar cells from various RGS source materials with different diffusion lengths were processed including an Al-gettering step which led to improved cell parameters. A $V_{oc}$ of 526 mV and fill factors of up to 73.3% were obtained for untextured solar cells resulting in an efficiency of $\eta = 9.5\%$. A dicing saw mechanically V-grooved RGS solar cell showed a record efficiency of 10.0%. Further studies and material improvements are expected to lead to higher efficiencies in the near future.
**Keywords:** Ribbons - 1: Characterisation - 2: Gettering - 3

## INTRODUCTION

In order to reduce the cost of Si photovoltaics big efforts have been undertaken to produce and investigate alternatives to mono- and cast multicrystalline silicon such as ribbon silicon, which is a very promising candidate. Its great advantage is the very fast production process without any material losses related to wafer cutting. RGS silicon shows altered physical properties as compared to standard silicon material mainly because of impurities present after ribbon growth. Therefore one route to improve the present material quality is the use of gettering steps during solar cell processing in order to produce cells with sufficient efficiencies.

## 1 RGS MATERIAL CHARACTERISATION

### 1.1 Transmission Electron Microscopy Studies

The number of defects is strongly affected by the temperature ramp used during cooling-down. We measured a crystal grain orientation dependent dislocation density of $10^5$-$10^7$ $cm^{-2}$ in RGS using Secco etching [2]. For a direct analysis of defects TEM (**T**ransmission **E**lectron **M**icroscope) studies were carried out, which confirmed the above mentioned dislocation density. In Fig. 1 a plan view TEM image of an older RGS sample with a nonoptimised temperature ramp is shown. A large number of stacking faults (SF) and dislocations (D) are visible, most of them being partial dislocations originating at the end of or in a stacking fault. In recent RGS material with an optimised temperature ramp less of these extended crystal defects are present. In Fig. 2 (same sample as in Fig. 1) a small angle grain boundary (GB) and several dislocations (D) are visible. Following the dislocation like a shadow a number of dislocation loops (L) can be seen. We think, that these loops originate during the movement of the dislocation through the crystal at higher temperatures under the influence of stress present. During the movement two effects can occur:

a) The dislocation can act as a sink for impurities and 'collect' foreign atoms along its way until its mobility is reduced so far locally, that a formation of a dislocation loop is energetically favourable.
b) The dislocation is pinned at agglomerated impurities where the velocity of the dislocation is reduced and arcs are formed resulting in dislocation loops during further movement.

In Fig. 2 a locally pinned dislocation (D') is visible. In between the first row of loops (L') and the dislocation

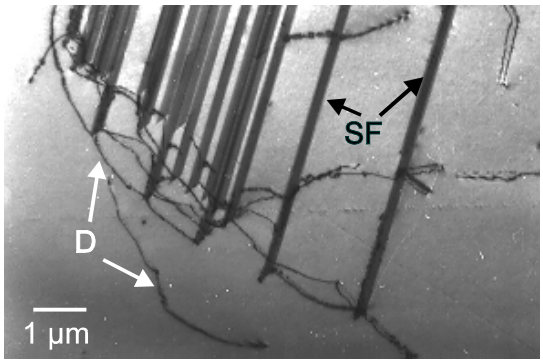


**Figure 1:** *Plan view TEM image of an older RGS sample containing stacking faults using the (220) reflex.*

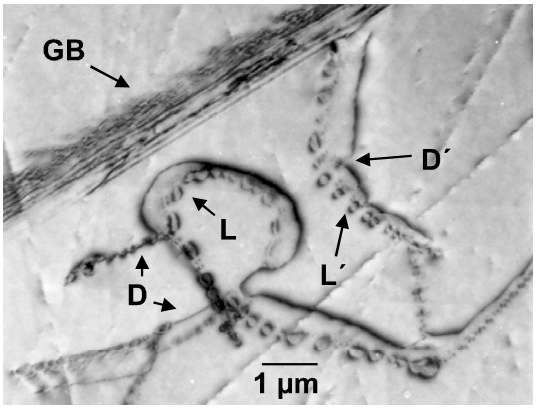


**Figure 2:** *Plan view TEM image showing dislocation loops and pinned dislocations using the (220) reflex.*

numerous smaller loops are observed in weaker contrast. These loops can arise when the dislocation moves on and is pinned again.

### 1.2 Surface Photovoltage Measurements

For the determination of the minority carrier diffusion length ($L_{diff}$) SPV (**S**urface **P**hoto**V**oltage) measurements were carried out which require a detailed knowledge of the absorption coefficient $\alpha(\lambda)$. In Fig. 3 $L_{diff}$ is extracted as the intercept of the linear fit with the x-axis for various RGS samples [3]. Three different generations of RGS material are shown:

- RGS1 with an $L_{diff}$ of 26 µm is taken from the same wafer shown in Fig. 1 and 2. Solar cells from this material are characterised by a low $V_{oc}$.
- RGS2 shows an $L_{diff}$ of 142 µm which is in the range of standard cast multicrystalline Si and represents RGS material of the second generation with maximum values for $L_{diff}$ of up to 200 µm. The largely improved $L_{diff}$ leads to a higher $J_{sc}$ in processed solar cells in the range of standard multicrystalline Si but also to relatively low fill factors.
- RGS3 with a comparatively low $L_{diff}$ similar to RGS1 which represents the latest RGS generation. A lower $J_{sc}$ as compared to RGS2 is overcompensated by a higher fill factor and an increase in $V_{oc}$.

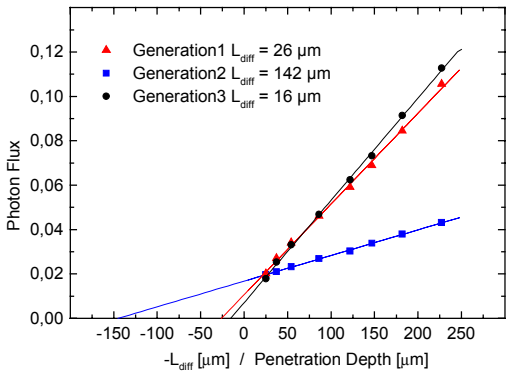


**Figure. 3:** *SPV measurements of three RGS samples representing different generations. $L_{diff}$ can be read from the interception of the linear fit with the negative x-axis.*

### 1.3 RGS Transport Properties

In order to investigate the RGS transport properties temperature dependent Hall measurements were carried out. In Fig. 4 the majority charge carrier concentration of two differently B doped RGS samples is shown. The ionization energies of 55 and 57 meV deduced from the linear fit shown (assuming an uncompensated behaviour) are in relatively good agreement with the literature value of 45 meV for Boron.

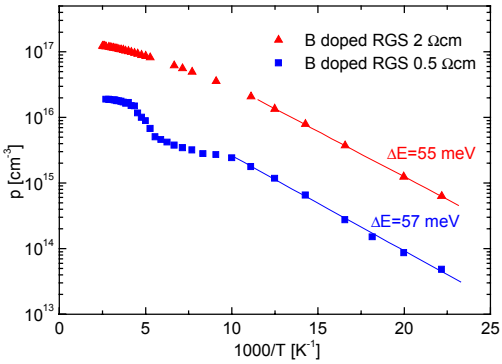


**Figure 4:** *Temperature dependent majority charge carrier concentration of differently B doped RGS samples.*

The lower doped sample shows a deviation from the conventional behaviour in the temperature range between 170 and 250 K. A likely mechanism is a defect related partial Fermi level pinning (or at least a restricted Fermi level movement in that temperature range) [4]. These defects maybe related to impurities such as metals or oxygen. For the latter a concentration above $10^{18}$ $cm^{-3}$ has been determined in FTIR measurements.

For temperatures exceeding 350 K the Hall mobilities µ(T) of the two RGS samples of Fig. 5 (identical with those of Fig. 4) are apparently determined by acoustic phonon scattering with an approximated $T^{-1.5}$ dependence. For lower temperatures a deviation from the normal temperature behaviour of monocrystalline FZ Si is visible. This anomaly results in a minimum for µ(T) at a certain temperature, which depends on the dopant concentration. This behaviour is typical for small grained multicrystalline Si [5] and could be explained with acceptor like traps in

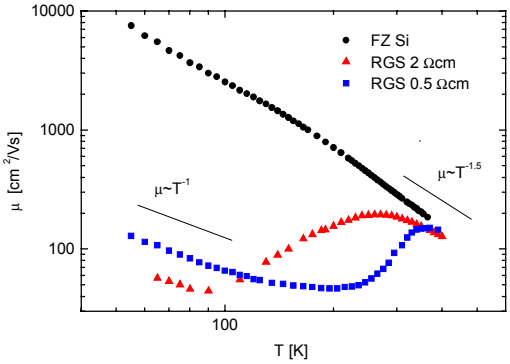


**Figure 5:** *Hall mobilities of two differently B doped RGS samples with anomalous temperature behaviour.*

grain boundaries causing a bending of the energy bands as proposed in [6].

## 2 RGS SOLAR CELLS

### 2.1 Process Sequence

Apart from the characterisation of the RGS as grown material RGS solar cells were processed at the new solar cell pilot line facility of the University of Konstanz. Fig. 6 shows the solar cell process sequence used. A levelling of the RGS wafers by mechanical abrasion is advantageous with respect to further processing due to the particular surface morphology of RGS and because of the possibility of removing an about 25 µm thick oxygen and impurity rich layer. In order to further remove impurities from the bulk of the material we investigated the effect of Al- and P-gettering. While no improvements were found yet using P-gettering, Al-gettered solar cells showed an increase in $V_{oc}$ of up to 19 mV in comparison to ungettered cells.

Planarisation with a levelling wheel

Saw damage etching

$POCl_3$ emitter diffusion

Thermal oxide passivation

Al gettering

Photolithography

Ti/Pd/Ag front contact evaporation

Lift-off

Al rear contact evaporation

$Si_3N_4/SiO_2$ DARC

Sintering

**Figure 6:** *Process sequence for RGS solar cells.*

### 2.2 Spectral Response Results

In spectral response measurements the largely enhanced $L_{diff}$ for RGS Si of the second generation is also visible. Fig. 7 shows the absolute IQE (**I**nternal **Q**uantum **E**fficiency) of an ungettered and two Al-gettered RGS solar cells. The strongly enlarged IQE in the long wavelength region leads to a $J_{sc} > 22$ mA/cm$^2$ without DARC for one Al-gettered solar cell. In order to obtain information on $L_{diff}$ from the spectral response data a linear fit has been carried out in the near infrared wavelength region (890-970 nm) according to the method proposed by Basore [7]. From this fit an effective diffusion length $L_{eff}$ can be obtained. For a rough estimation of the actual $L_{diff}$ we assumed the back surface recombination velocity to be $10^7$ cm/s and used a diffusion constant of 31 cm$^2$/s. An $L_{diff} = 26$ µm was obtained for an ungettered solar cell as compared to 90 and 202 µm for gettered cells. The latter values are similar to those of standard cast multicrystalline Si material. At about 600 nm a detector changeover has led

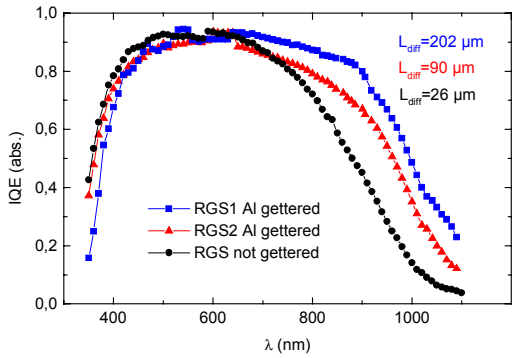


**Figure 7:** *Spectral response data showing the absolute internal quantum efficiencies for an ungettered and two Al-gettered RGS solar cells.*

to an erratic signal.

The efficiency η for this second generation is limited by the relatively low values for both fill factor and $V_{oc}$. We focused on improving $V_{oc}$ because we could demonstrate a strong relationship between a large fill factor and a high $V_{oc}$. Moreover, a combination of a high $J_{sc}$ and a low fill factor was noticed. The latest third generation of RGS shows higher fill factors and an increased $V_{oc}$ due to less metal impurities present. It is still not understood at the moment why a reduction of metal impurities in the third RGS generation leads to a lower $L_{diff}$. Unfortunately, it is yet not possible to combine the best $L_{diff}$ with a high $V_{oc}$ (and therefore a high fill factor).

### 2.3 I-V-Results

In Fig. 8 the IV-characteristics of an RGS solar cell are shown. On this cell a $V_{oc}$ of 526 mV, to our knowledge the highest value for RGS Si, could be measured. We could demonstrate that a $Si_3N_4/SiO_2$ PECVD-DARC (**P**lasma **E**nhanced **C**hemical **V**apour **D**eposition - **D**ouble **A**nti**R**eflection **C**oating) is responsible for a raise of $V_{oc}$, possibly because of the passivation properties of hydrogen indiffusion during the deposition and an improved surface passivation. This improvement (13 mV in Fig. 8) can be further increased by a following annealing step as visible

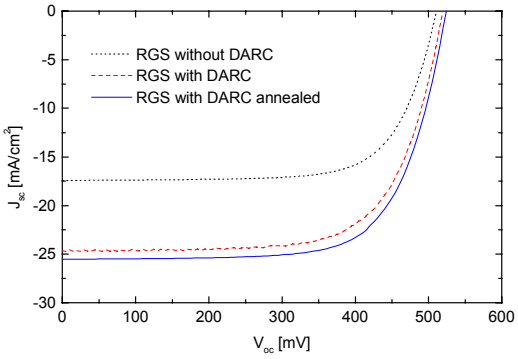


**Figure 8:** *Illuminated IV-characteristics of a RGS solar cell before and after a PECVD-DARC and a following annealing step.*

in Fig. 8. The still relatively low $V_{oc}$ compared to standard multicrystalline Si is in our opinion caused either by metal impurities or by oxygen, aggregating at extended crystal defects like grain boundaries, stacking faults or dislocations. For the possible impact of oxygen on the diode characteristics see [8].

### 2.4 V-grooved Solar Cells

Textured solar cells show less reflection and a higher charge carrier collection probability. Both effects lead to an increased $J_{sc}$. Multicrystalline Si solar cells can be textured by a mechanical V-grooving using a conventional dicing saw [9]. This technique was applied to the latest RGS material and resulted in a reduced reflection for a V-grooved cell as shown in Fig. 9.

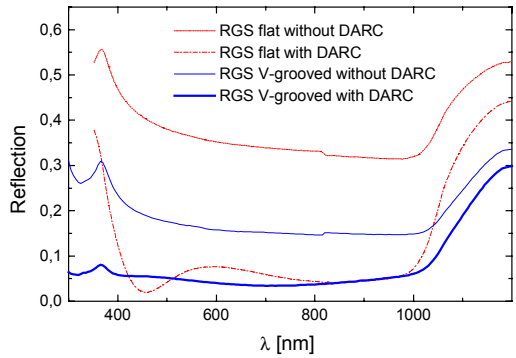


**Figure 9:** *Comparison of the total reflection of an untextured and a mechanically V-grooved RGS solar cell before and after DARC respectively.*

Tab. I gives the obtained cell parameters for both an untextured and a mechanically V-grooved RGS solar cell. As expected by computer simulations [10] the mechanical texturing leads to an increase in $J_{sc}$ and a slightly lower $V_{oc}$ as compared to a similar untextured cell. On the V-grooved cell we reached an efficiency of $\eta = 10.0\%$, the highest value reported to date for an RGS solar cell.

**Table I:** *Solar cell data for an untextured and a mechanically V-grooved RGS solar cell.*

| | **Untextured** | **V-grooved** |
|---|---|---|
| **$V_{oc}$ [mV]** | 526 | 517 |
| **$J_{sc}$ [mA/cm$^2$]** | 26.1 | 27.1 |
| **FF [%]** | 69.2 | 71.2 |
| **η [%]** | 9.5 | **10.0** |

## CONCLUSIONS

With RGS a new and promising multicrystalline Si material for solar cell applications was presented. Secco etching and TEM showed a relatively high crystal defect concentration (dislocation density $10^5$-$10^7$ cm$^{-2}$) and a grain diameter of about 0.5 mm which leads to anomalous temperature dependent Hall mobilities. These anomalies are likely to result from acceptor like traps located at extended crystal defects like grain boundaries. The oxygen concentration measured with FTIR-spectroscopy is above $10^{18}$ cm$^{-3}$.

Three generations of RGS material were under investigation. The second shows diffusion lengths of up to 200 µm which is in the range of standard cast multicrystalline Si and results in a $J_{sc}$ of more than 22 mA/cm$^2$ before DARC. These large values of $L_{diff}$ could also be demonstrated by spectral response analysis. In the third generation less impurities are present and therefore a higher $V_{oc}$ is obtained. A strong relationship between a high $V_{oc}$ and a high fill factor has been observed on one side and a combination of a high $J_{sc}$ and a low fill factor on the other. At the moment it is not understood why less impurities in the latest generation are resulting in a better $V_{oc}$ but smaller diffusion lengths as compared to the second generation.
Material of the third generation shows a $V_{oc}$ of up to 526 mV, fill factors of up to 73.3% and a V-grooved RGS solar cell shows an efficiency of $\eta = 10.0\%$ due to less reflection and a higher charge carrier collection probability. Further improvements in RGS production, optimised gettering techniques and the use of hydrogen passivation should lead to better results in the near future.

## ACKNOWLEDGEMENTS

We like to thank Dr. F. Pillipp at the MPI-MF Stuttgart for the possibility of TEM experiments and M. Keil for technical assistance during solar cell processing. This work was supported by the German BMBF under contract number 0329557A and within the JOULE program of the European Commission under contract number JOR3-CT 95-0030.

## REFERENCES

[1] H. Lange, I. A. Schwirtlich: *J. Cryst. Growth* **104** (1990) 108
[2] F. Secco*: J. Electrochem. Soc*. **119** (1972) 948
[3] A. M. Goodman: *J. Appl. Phys.* **32** (1961) 2550
[4] H. Nussbaumer, F. P. Baumgartner, G. Willeke, E. Bucher: *submitted for publication*
[5] P. Fath, G. Hahn: *to be published*
[6] H. Nussbaumer: *PhD-Thesis*, Universität Konstanz (1996)
[7] P. A. Basore: *Proc. 23rd IEEE Photovoltaic Spec. Conf.,* Louisville (1993) 147
[8] J. Vanhellemont, E. Simoen, A. Kaniava, M. Libezny, C Claeys: *J. Appl. Phys.* **77** (11) 5669
[9] G. Willeke, H. Nussbaumer, H. Bender, E. Bucher: *Solar Energy Materials and Solar Cells* **26** (1992) 345
[10] C. Zechner, P. Fath, G. Willeke, E. Bucher: *this conference*